Strain Analysis of Ridges on Europa

Sophia Zipparo, Karla Núñez, Laurent Montési, Samuel Howell (JPL)

GEOL 394

Jet Propulsion Laboratory
California Institute of Technology

University of Maryland

Background

Jupiter's moon Europa has a global subsurface ocean beneath an icy shell, which may host an environment in which life develop. Europa experienced recent geologic resurfacing, in part through globally distributed linear ridges, which include double ridges and ridge complexes. Some proposed methods of double ridge formation include incremental ice wedging (Melosh and Turtle, 2004), a crystallizing water intrusion (Johnston and Montési, 2014), or heating caused by repeated strike-slip motion on a vertical fault (Nimmo and Gaidos, 2002).

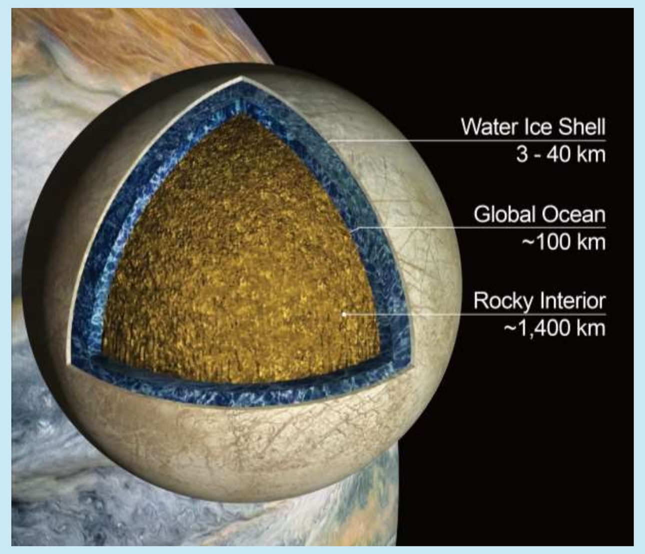

Figure 1: Global structure of Europa (Howell & Pappalardo, 2020)

Head et al. (2009) proposed that double ridges and ridge complexes evolved from a simple crack into progressively more complex structures, including double ridges and ridge complexes. Here, we explore whether the morphologies of double ridges and ridge complexes may be the result of the magnitude of strain and the strain regime and how that may relate to potential formation mechanisms.

Hypothesis

Strain controls the difference between ridge morphologies.

Methods

Five ridges in two regions were mapped using a global mosaic of Galileo images from the USGS (Figures 3 and 4). At each ridge, multiple background features crossed by the ridge were identified. The angle of these background features, θ, the total width of the ridge, Y, and the total offset, X, were measured. Using the geometry described in Figure 2, we derive the equation:

$$X = y_0 * \tan(\theta) + dx.$$

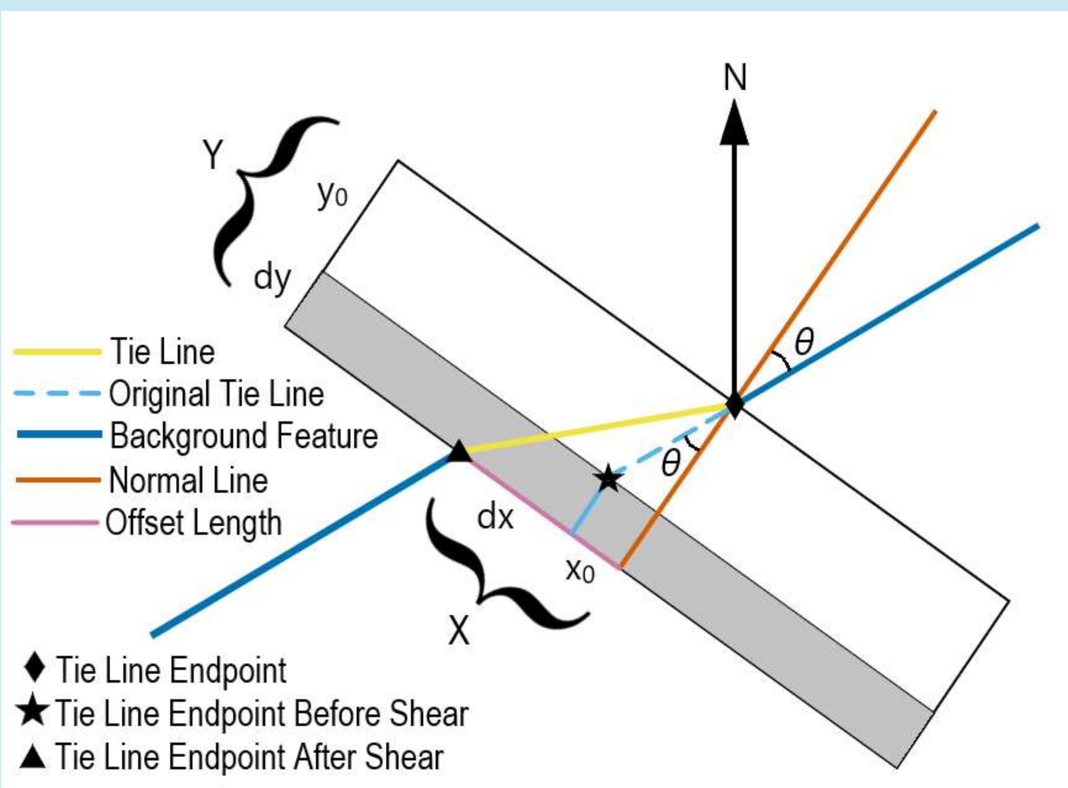

Figure 2: Geometry of a deforming ridge, where dark blue is a background feature at angle θ from normal (orange). This angle, projected across the ridge (light blue line) causes offset x_0. Total offset, X, equals x_0 plus shear offset, dx. Total width of the ridge, Y, equals initial width, y_0, plus extension, dy.

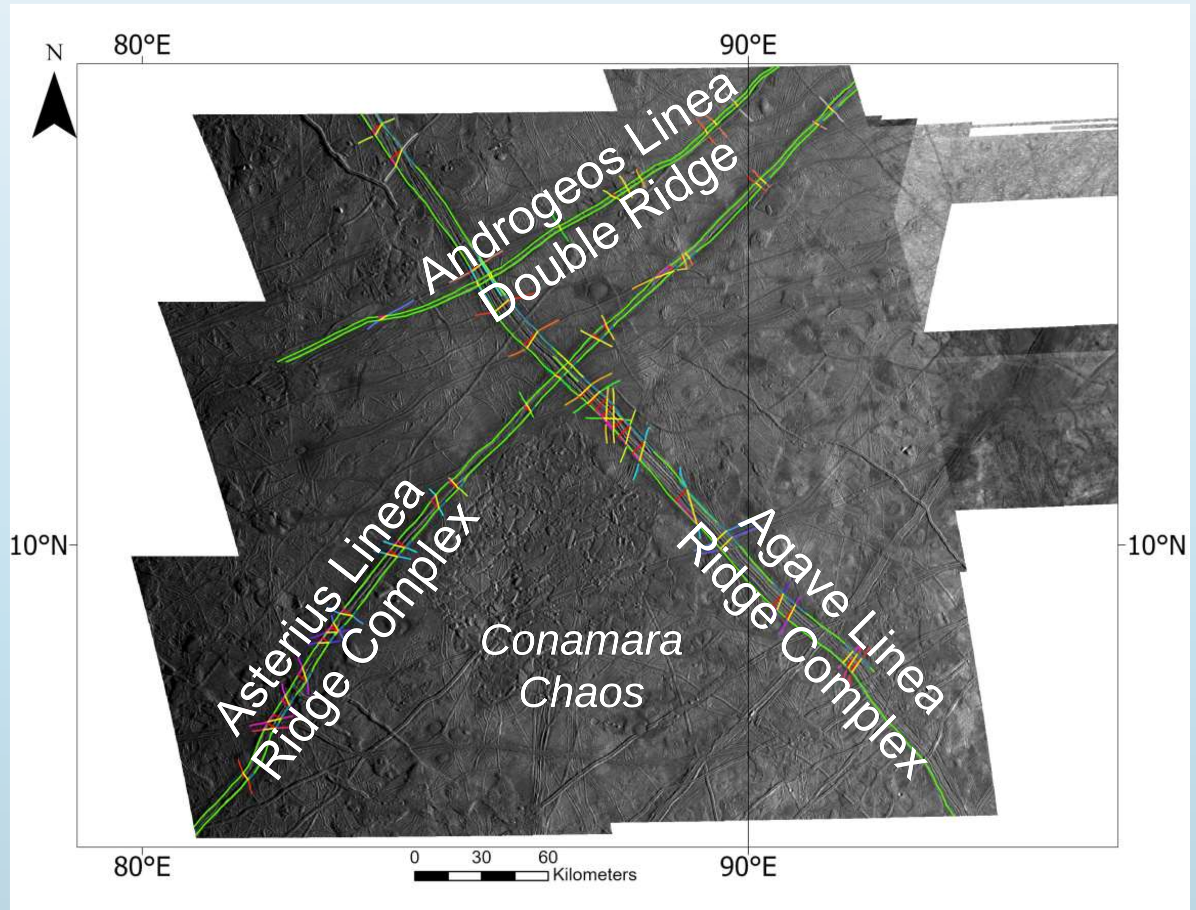

Figure 3: Mapping of the region near Conamara Chaos, including the ridge complexes Agave Linea and Asterius Linea, as well as the double ridge Androgeos Linea.

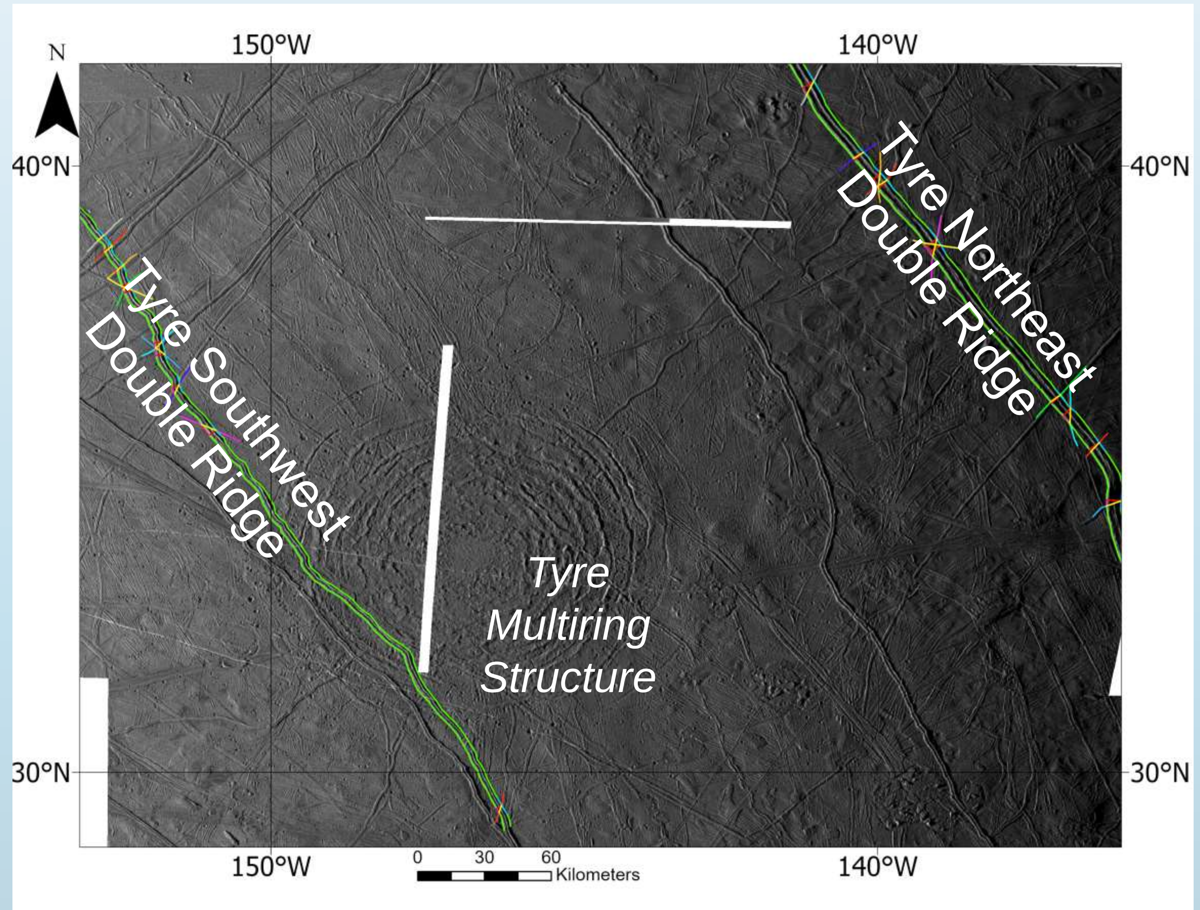

Figure 4: Mapping of the region near the Tyre Multiring Structure, including two unnamed double ridges, one in the northeast and the other in the southwest.

Results

From our measurements of θ, Y, and X, we plot our data for each background feature (Figure 5). For each ridge, we produce a linear fit. The slope of the best fit line gives the initial width of the ridge (y_0), and the intercept gives the shear offset (dx). For each ridge, we calculate the average ridge width (Y_{av}). From there, we calculate the extension, $dy = Y - y_0$. The shear strain (γ) is calculated using the equation $\gamma = \frac{dx}{y_0}$. Normal strain is calculated using the equation $\varepsilon = \frac{dy}{y_0}$. These numbers are reported in Table 1. A comparison of both normal and shear strains to the average ridge width (Figure 6) shows that shear strain is not significantly different from zero. There is some non-zero amount of extension evidenced by normal strain, but the extension (dy) is not enough to explain the average width (Y_{av}).

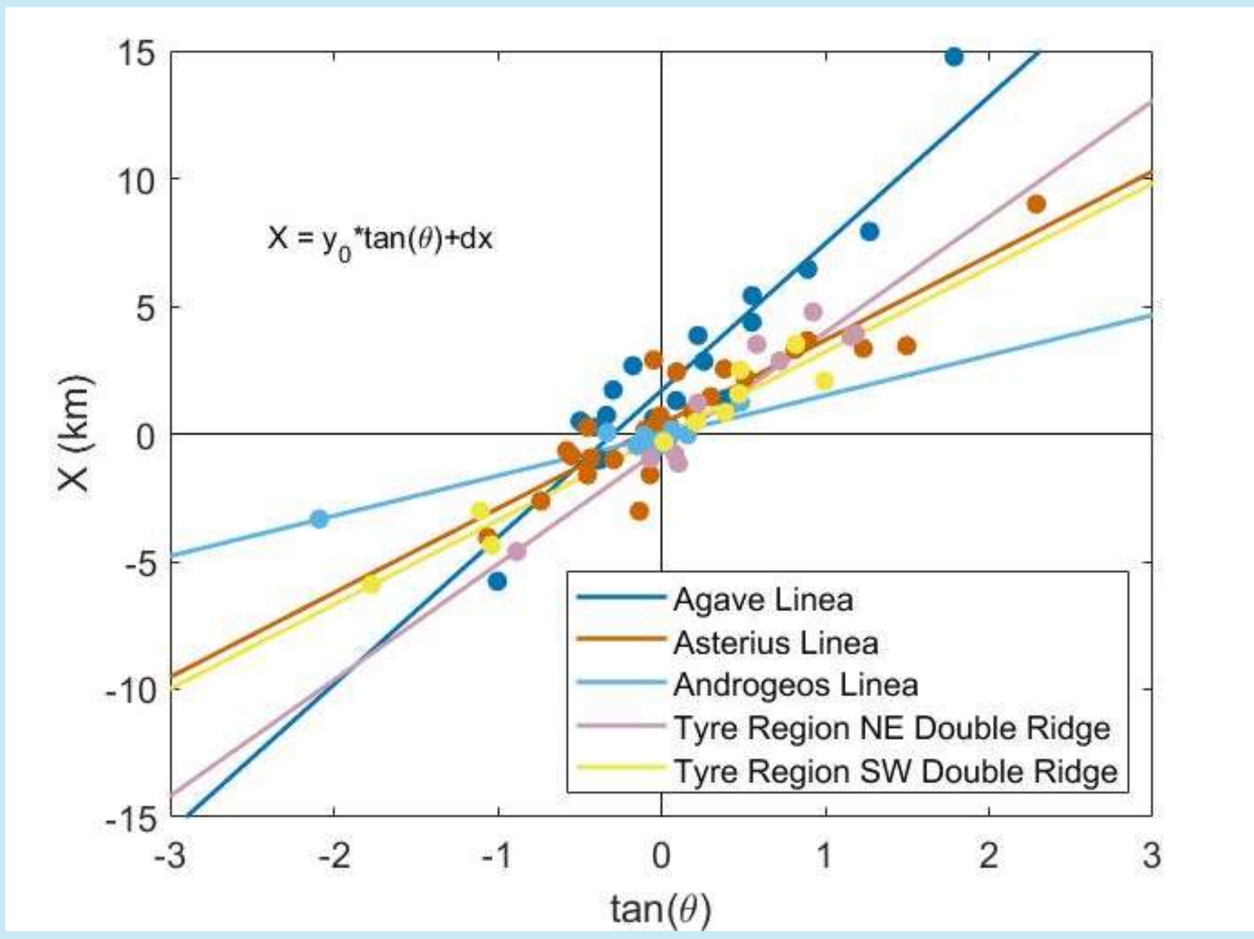

Figure 5: Data showing the linear relationship between total offset and $\tan(\theta)$. Each point represents the crossing of a background feature. The slope of the best fit line is the initial width, y_0 and the intercept is the shear offset, dx.

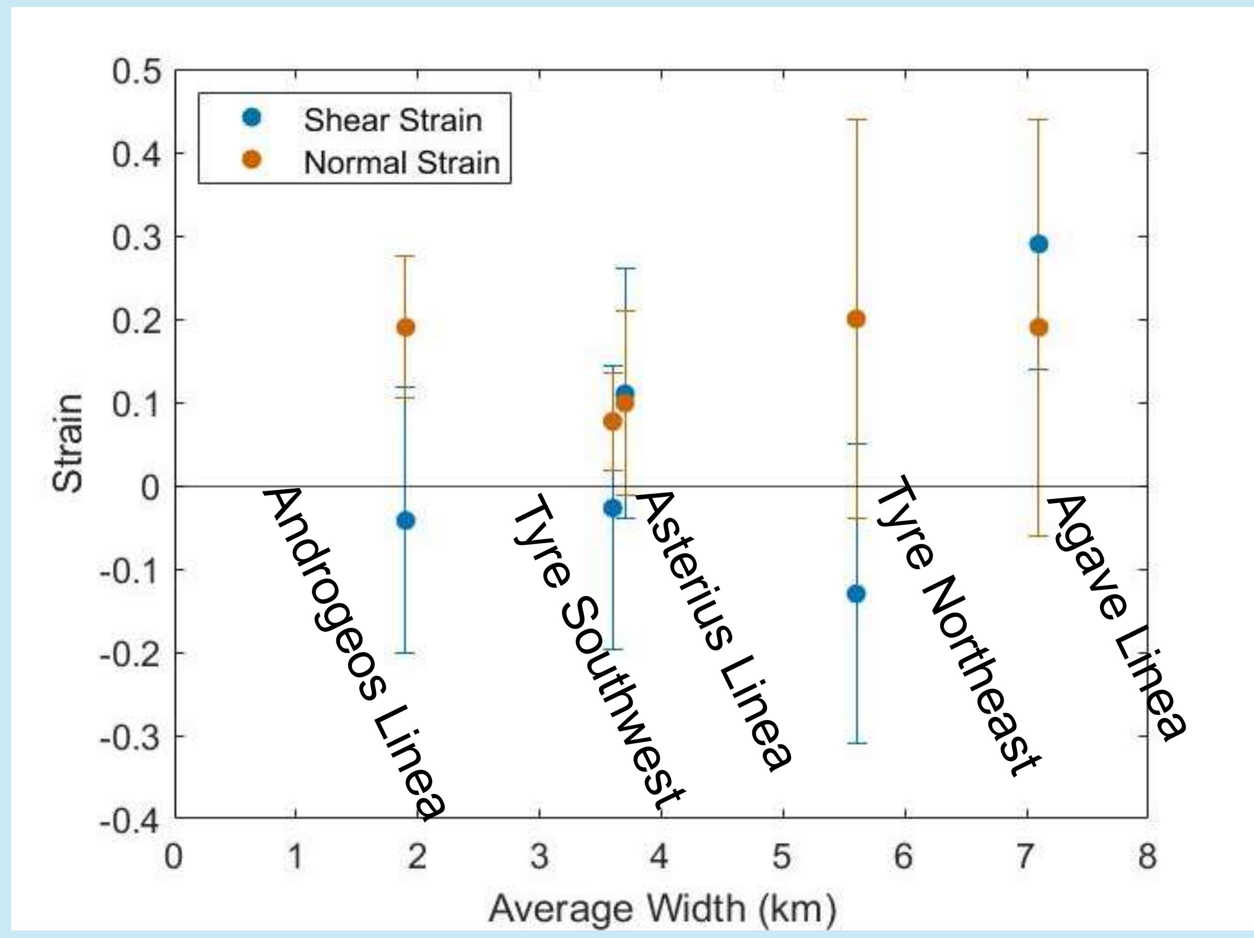

Figure 6: Results of normal and shear strains compared to average ridge width. For shear strain, positive values indicate left-lateral motion, and negative right-lateral. For normal strain, positive values indicate extension and negative contraction

Table 1: Data calculated for each ridge based on measurements and ridge geometry from Figure 2. Initial width (y_0), shear offset (dx), average width (Y_{av}), and extension (dy) are measured in km. Normal strain (ε) and shear strain (γ). Uncertainties are derived from standard deviations (Y_{av}), the linear fit (y_0 and dx), and error propagation (dy, ε, and γ).

Ridge	Type of Ridge	y_0	dx	Y_{av}	dy	ε	γ
Agave Linea	Ridge Complex	5.8 ± 1.2	1.7 ± 0.77	7.1 ± 0.54	1.4 ± 1.8	0.19 ± 0.25	0.29 ± 0.15
Asterius Linea	Ridge Complex	3.3 ± 0.66	0.38 ± 0.49	3.7 ± 0.85	0.36 ± 0.39	0.1 ± 0.11	0.11 ± 0.15
Androgeos Linea	Double Ridge	1.6 ± 0.39	-0.07 ± 0.26	1.9 ± 0.19	0.37 ± 0.16	0.19 ± 0.09	-0.04 ± 0.16
Tyre Northeast	Double Ridge	4.5 ± 1.1	-0.57 ± 0.82	5.6 ±0.53	1.1 ± 1.4	0.2 ± 0.24	-0.13 ± 0.18
Tyre Southwest	Double Ridge	3.3 ± 0.63	-0.09 ± 0.55	3.6 ± 0.44	0.27 ± 0.21	0.08 ± 0.06	-0.03 ± 0.17

Discussion & Conclusions

Similar work using geometric analysis to determine shear offsets and dilation has been done by Culha et al. (2014) and Coulter (2009). Both analyzed similar ridges, enabling a direct comparison to my work (Figure 7). The majority of our calculations aligned, with the exception of Culha et al. (2014) finding contraction associated with the Tyre Southwest double ridge where we find extension. The main difference between our analyses is that they assume ridges form from a crack with no initial width; we do, allowing for a broader range of possible formation mechanisms.

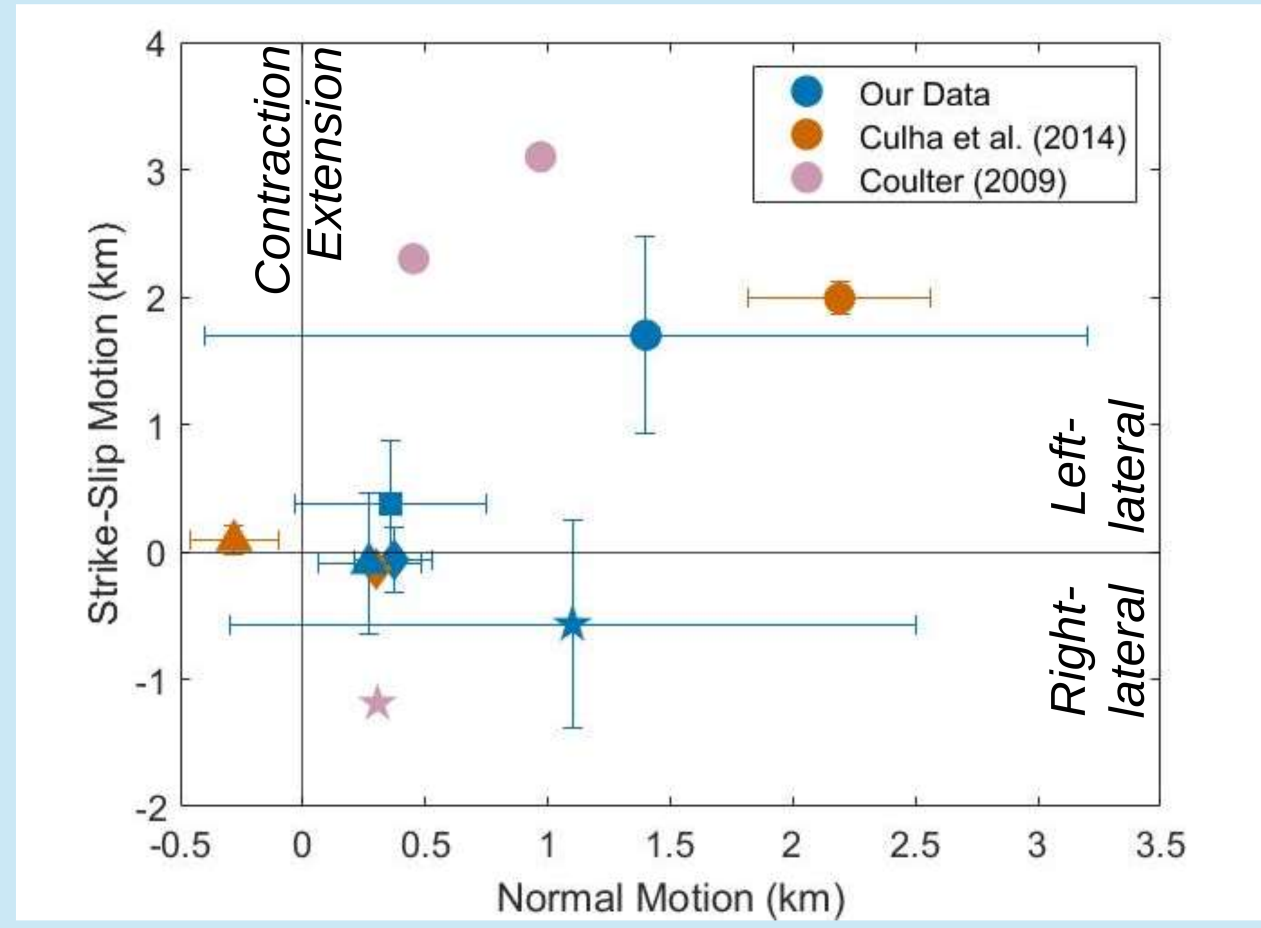

Figure 7: Comparison of the data to analyses by Culha (2014) and Coulter (2009). Circles represent Agave Linea, squares Asterius Linea, diamonds Androgeos Linea, stars Tyre Northeast, and triangles Tyre Southwest.

There seem to be variable amounts of shear and normal motion. Since neither shear nor normal strain can explain the total width of observed ridges, there must be deformation occurring in place, called overprinting. This conclusion aligns with models of formation mechanisms, such as subsurface water intrusions or warm diapirs, that indicate subsurface water transport. The potential transport of liquid water could mean that evidence of life, if present on Europa, could be found at ridges by a future mission.

Acknowledgements & References

Portions of this work were carried out at the Jet Propulsion Laboratory, California Institute of Technology, under contract with the National Aeronautics and Space Administration (Solar System Workings grant #80NM0018F0612).

Howell, S.M., Pappalardo, R.T., 2020. NASA's Europa Clipper — a mission to a potentially habitable world. Nat. Commun. 11, 1311.

Melosh, H.J., Turtle, E.P., 2004. Ridges on Europa: Origin by Incremental Ice- Wedging. Lunar Planet. Sci. XXXV. Abstract #2029

Johnston, S., Montési, L., 2014. Formation of ridges on Europa above crystallizing water bodies inside the ice shell. Icarus 237, 190-201.

Nimmo, F., Gaidos, E., 2002. Strike-slip motion and double ridge formation on Europa. J. Geophys. Res. Planets 107, 5-1-5-8.

Culha, C., Hayes, A.G., Manga, M., & Thomas, A.M., 2014. Double ridges on Europa accommodate some of the missing surface contraction. J. Geophys. Res. Planets 119, 395-403.

Head, J., Pappalardo, R, Sullivan, R., 1999. Europa: Morphological characteristics of ridges and triple bands from Galileo data (E4 and E6) and assessment of linear diapirism model. J. Geophys. Res. Planets 104, 24223-24236.

Coulter, 2009. Kinematic and morphological evolution of Europa's ridges (unpublished master's thesis). University of Idaho.